

# Neutron capture cross section of $^{14}\text{C}$ of astrophysical interest studied by Coulomb breakup of $^{15}\text{C}$

T. Nakamura,<sup>1</sup> N. Fukuda,<sup>2</sup> N. Aoi,<sup>2</sup> N. Imai,<sup>3</sup> M. Ishihara,<sup>2,4</sup> H. Iwasaki,<sup>4</sup> T. Kobayashi,<sup>5</sup> T. Kubo,<sup>2</sup> A. Mengoni,<sup>2,6</sup> T. Motobayashi,<sup>2</sup> M. Notani,<sup>7</sup> H. Otsu,<sup>2</sup> H. Sakurai,<sup>2</sup> S. Shimoura,<sup>7</sup> T. Teranishi,<sup>7</sup> Y. X. Watanabe,<sup>3</sup> and K. Yoneda<sup>2</sup>

<sup>1</sup>*Department of Physics, Tokyo Institute of Technology, 2-12-1 O-Okayama, Tokyo 152-8551, Japan*

<sup>2</sup>*RIKEN Nishina Center for Accelerator-Based Science, 2-1 Hirosawa, Wako, Saitama 351-0198, Japan*

<sup>3</sup>*IPNS, KEK, 1-1 Oho, Tsukuba, Ibaraki 305-0801, Japan*

<sup>4</sup>*Department of Physics, University of Tokyo, Hongo 7-3-1, Bunkyo, Tokyo 113-0033, Japan*

<sup>5</sup>*Department of Physics, Tohoku University, 2-1 Aoba, Aramaki, Aoba, Sendai 980-8578, Japan*

<sup>6</sup>*International Atomic Energy Agency (IAEA), NAPC/Nuclear Data Section, P. O. Box 100, Wagramer Strasse 5, A-1400 Vienna, Austria*

<sup>7</sup>*Center for Nuclear Study, University of Tokyo (CNS) RIKEN Campus, 2-1 Hirosawa, Wako, Saitama 351-0198, Japan*

(Received 26 January 2009; published 20 March 2009)

The neutron capture reaction on  $^{14}\text{C}$  leading to the  $^{15}\text{C}$  ground state, which plays an important role in various nucleosynthesis processes, has been studied using the Coulomb breakup of  $^{15}\text{C}$  on a Pb target at 68 MeV/nucleon. The breakup cross section has been converted into the energy-dependent neutron capture cross section using the principle of detailed balance. The energy spectrum shows typical  $p$ -wave neutron capture characteristics, which is explained by the fact that the ground state of  $^{15}\text{C}$  possesses a strong single-particle  $s$ -wave component and a moderate-sized neutron halo structure. The capture cross section for the  $^{14}\text{C}(n, \gamma)^{15}\text{C}$  reaction derived from the present experiment has been found to be consistent with the most recent data, directly measured using a  $^{14}\text{C}$  target. This result assures the validity of the Coulomb breakup method in deriving the neutron capture cross section for neutron-rich nuclei.

DOI: [10.1103/PhysRevC.79.035805](https://doi.org/10.1103/PhysRevC.79.035805)

PACS number(s): 21.10.Jx, 25.60.Gc, 26.30.Hj, 27.20.+n

## I. INTRODUCTION

The neutron capture by  $^{14}\text{C}$  has drawn much attention due to its importance in several nucleosynthesis processes. Wiescher *et al.* [1] discussed the neutron induced CNO cycle,  $^{14}\text{C}(n, \gamma)^{15}\text{C}(\beta^-)^{15}\text{N}(n, \gamma)^{16}\text{N}(\beta^-)^{16}\text{O}(n, \gamma)^{17}\text{O}(n, \alpha)^{14}\text{C}$ , which occurs in the burning zone of asymptotic giant branch (AGB) stars with 1–3  $M_{\odot}$ . The reaction  $^{14}\text{C}(n, \gamma)^{15}\text{C}$  is the slowest in this reaction chain, and thus controls the cycle.

This reaction can also be important for the synthesis of heavier elements. Terasawa [2,3] proposed an  $r$ -process initiating from the lightest elements, and thus containing light neutron rich nuclei in the path. This new  $r$  process was inferred from the similarity of the nuclear abundance pattern in metal-deficient halo stars to that of ordinary ones. The neutron capture of  $^{14}\text{C}$  lies in one of the critical reaction flows of this process.

Another possible important role for the neutron capture of  $^{14}\text{C}$  has been suggested in the framework of inhomogeneous big bang models, where the neutron-rich zone induces the nucleosynthesis and reaction paths involving light neutron-rich nuclei can appear. In this scenario, the  $^{14}\text{C}(n, \gamma)^{15}\text{C}$  reaction is again considered to be one of the key reactions [4].

From the nuclear structure point of view, the ground state of  $^{15}\text{C}$ , i.e., the final state of the capture reaction, is intriguing because it has a moderate-sized neutron halo with a neutron separation energy  $S_n$  of only 1.218 MeV and with the wave function of the valence neutron extending far out of the  $^{14}\text{C}$  core. The main configuration of the  $^{15}\text{C}$  ground state is  $^{14}\text{C}(0^+) \otimes \nu 2s_{1/2}$ , which facilitates the formation of the neutron halo because of the absence of the centrifugal barrier for the  $s$ -wave neutron. The capture of a  $p$ -wave neutron [5] is then expected to become the dominant process in the present

case since the final state is predominantly the  $s$  orbital and the associated  $\gamma$ -ray is  $E1$  dominant. Such a case is rather exceptional as the neutron capture process in stellar reactions usually occurs for  $s$ -wave neutrons and the cross section obeys the  $1/v$  law. The dominance of the  $p$ -wave neutron capture has been observed for stable nuclei, where the final state can be an excited state in the  $s$  orbital [6,7]. Note that for the current reaction the final state of the capture reaction is the ground state.

In spite of such importance both in astrophysics and nuclear structure, there has been controversy in the previous experimental results for this neutron capture process. The pioneering experiment to extract the  $^{14}\text{C}(n, \gamma)^{15}\text{C}$  reaction rate was made by a direct measurement of neutron capture cross section on a  $^{14}\text{C}$  radioactive target [8]. The extracted MACS (Maxwellian averaged capture cross section) of  $1.72 \pm 0.43 \mu\text{b}$  at  $kT = 23 \text{ keV}$  was about a factor of 4–5 smaller than predicted by the  $p$ -wave direct neutron capture calculations [4,9]. Recently, Horváth *et al.* measured the Coulomb breakup of  $^{15}\text{C}$  at 35 MeV/nucleon at MSU [10], and found that the energy spectrum of the inverse capture reaction is very different from the expected  $p$ -wave behavior. Their extracted capture cross section was about twice as large as that from the mentioned direct measurement. More recently, Datta Pramanik *et al.* measured the Coulomb breakup at higher energies, 605 MeV/nucleon at GSI [11]. The result showed a typical direct breakup spectrum, which indicates that the  $p$ -wave direct capture is dominant for the inverse reaction. The GSI result provided an even higher value for the capture cross section: as much as about four times the value of the first direct measurement.

Most recently, a direct capture measurement was performed again by Reifarth *et al.* [12], showing a significantly higher

cross section compared to the first measurement, a result consistent with the direct capture model prediction. Note that in this new measurement, an energy spectrum ranging from  $\sim 10$  keV–800 keV was also obtained so that a direct comparison to the Coulomb breakup energy spectrum is now possible. We stress that the present case is a rare case where the energy spectra of both, neutron capture and Coulomb breakup, can be measured. In fact, recent reaction theories [13,14] treating breakup reactions can also be tested using the measurements of both, direct and inverse reaction channels.

Part of the current experimental results were shown as preliminary data in a short conference report [15]. The present article presents the final experimental results in full details. The energy spectra of the breakup cross section for different angular cuts, the  $B(E1)$  spectrum, and the extracted neutron capture cross section of  $^{14}\text{C}$  are extracted and presented here. From the energy spectra of the breakup cross section, we extract the spectroscopic factor for  $^{14}\text{C}(0^+) \otimes \nu 2s_{1/2}$  (halo configuration) and compare it with previously extracted values from different reactions and parameter sets. The spectroscopic factor of the weakly-bound  $^{15}\text{C}$  ground state is important as a reference point in the systematic study of reduction of the spectroscopic strength, dependent on nucleon binding energies [16,17]. The  $B(E1)$  excitation spectrum of  $^{15}\text{C}$  is used to estimate the size of the halo. Finally, the energy dependence of the capture cross section is compared to previous experimental results. We also discuss the effect of a possible resonance state at  $E_{\text{c.m.}} = 1.885$  MeV in  $^{15}\text{C}$  ( $E_{\text{c.m.}}$  denotes the  $n-^{14}\text{C}$  center-of-mass energy), first introduced in Ref. [4].

We organize the paper as follows. Section II describes the Coulomb breakup as a tool to extract the neutron capture cross section. Section III describes the experimental procedure. Section IV presents the results of  $^{15}\text{C}$  Coulomb breakup and extracted neutron capture cross section, and compare those to the existing experimental data and theories. In Sec. V, the conclusions are given.

## II. COULOMB BREAKUP FOR EXTRACTING THE NEUTRON CAPTURE CROSS SECTION

Coulomb breakup of a fast radioactive projectile in the changing electromagnetic field of a high- $Z$  target can be a useful tool to extract information on the inverse radiative capture process. The Coulomb breakup reaction can be regarded as an inverse process of radiative capture reactions such as  $(n, \gamma)$ ,  $(p, \gamma)$ , and  $(\alpha, \gamma)$ . For instance, the  $^7\text{Be}(p, \gamma)^8\text{B}$  reaction process, which takes place in the sun and provides exclusively the high-energy neutrino flux measured in underground facilities such as Super-Kamiokande and SNO, has been successfully studied using the Coulomb breakup of  $^8\text{B}$  [18–20].

The Coulomb breakup process can be described by the semiclassical first-order perturbation theory of electromagnetic interaction [21,22]. The cross section for Coulomb breakup is expressed as a product of the  $E1$  virtual photon flux,  $N_{E1}(E_\gamma)$ , and the photo-absorption cross section,  $\sigma_{\gamma n}$ , as

in

$$\frac{d\sigma}{dE_{\text{rel}}} = \frac{16\pi^3}{9\hbar c} N_{E1}(E_\gamma) \frac{dB(E1)}{dE_{\text{rel}}} = N_{E1}(E_\gamma) \frac{\sigma_{\gamma n}(E_\gamma)}{E_\gamma}, \quad (1)$$

where  $B(E1)$  stands for the  $E1$  reduced transition probability and  $N_{E1}(E_\gamma)$  is the  $E1$  virtual photon number of  $\gamma$  rays with energy  $E_\gamma$ . The relative energy  $E_{\text{rel}}$  between the neutron and the core nucleus  $^{14}\text{C}$  is related to the excitation energy by  $E_x = E_{\text{rel}} + S_n$ . The excitation energy  $E_x$  is equivalent to  $E_\gamma$  in the Coulomb breakup process. This simple relation, based on the first-order perturbation theory, allows to extract the  $\sigma_{\gamma n}$  from the  $E_{\text{rel}}$  energy spectrum.

A nuclear breakup component can be mixed with the Coulomb breakup, acting as a possible background. Although the Coulomb breakup is estimated to be dominant for the current experiment, in order to obtain the Coulomb breakup component we adopt here an analysis method based on the selection of scattering angles. This method was successfully applied to the Coulomb breakup experiments of  $^{11}\text{Be}$  [23] and  $^{11}\text{Li}$  [24] at similar incident energies. The photon number  $N_{E1}(E_\gamma)$  is calculated as

$$N_{E1}(E_\gamma) = \int_0^{\theta_c} \frac{dn_{E1}(\theta, E_x)}{d\Omega} d\Omega, \quad (2)$$

where  $\theta_c$  denotes the cutoff angle and  $n_{E1}(\theta, E_x)$  is the photon number at  $\theta$  and  $E_x$ .

The obtained  $\sigma_{\gamma n}$  is then converted into  $\sigma_{n\gamma}$  using the principle of detailed balance

$$\sigma_{n\gamma}(E_{\text{c.m.}}) = \frac{2I_A + 1}{2I_{A-1} + 1} \frac{E_\gamma^2}{2\mu c^2 E_{\text{c.m.}}} \sigma_{\gamma n}(E_\gamma), \quad (3)$$

where  $I_A = 1/2$ , and  $I_{A-1} = 0$  for the present case, and  $\mu$  denotes the reduced mass of  $^{14}\text{C} + n$ .

An advantage of the Coulomb breakup as compared to direct capture experiments is a large gain factor in the reaction yield. With the detailed balance [Eq. (3)], one finds that the  $\sigma_{\gamma n}$  is larger by  $10^{3-4}$ , when compared to  $\sigma_{n\gamma}$ . An additional gain factor, due to the large number of virtual photons, is of the order of  $10^2$ . One should consider also the advantage of kinematic focusing and of the possibility of using a thick target of the order of  $100$  mg/cm $^2$ . Due to these factors, one can achieve a significantly higher yield in a Coulomb breakup experiment as compared to the case of a neutron capture reaction, even for a secondary beam experiment. We also note that in the case of the  $^{14}\text{C}(n, \gamma)^{15}\text{C}$  reaction, the neutron capture measurement requires a  $^{14}\text{C}$  radioactive sample, which needs extra care in handling.

The Coulomb breakup process does not cover all the possible reaction channels corresponding to a particular neutron capture reaction. In fact, the detailed balance can only be applied to the ground state transition. The neutron capture of  $^{14}\text{C}$  leads either to the ground state or to the first excited state at 0.74 MeV, the only bound excited state of  $^{15}\text{C}$ . However, the cross section for transitions leading to the first excited state of  $^{15}\text{C}$  is negligible compared to the cross section for the ground state reaction channel [4,9]. Therefore, the correspondence between the Coulomb breakup and the neutron capture processes is well established in the present case.

### III. EXPERIMENT

#### A. Experimental method

The  $^{15}\text{C}$  breakup spectrum is obtained applying the invariant mass method (see, for example, Refs. [23–27]). The  $^{14}\text{C} + n$  relative energy,  $E_{\text{rel}}$ , is obtained event-by-event from the invariant mass of the excited  $^{15}\text{C}$ , reconstructed from the momentum vector of outgoing  $^{14}\text{C}$ ,  $\mathbf{P}(^{14}\text{C})$ , and that of the neutron,  $\mathbf{P}(n)$ .

The scattering angle of the c.m. (center of mass) system of  $^{14}\text{C} + n$  can be measured as the opening angle  $\theta$  between the incident momentum vector  $\mathbf{P}(^{15}\text{C})$  and that of the outgoing  $^{14}\text{C} + n$  system,  $\mathbf{P}(^{14}\text{C}) + \mathbf{P}(n)$ , in the c.m. frame of  $^{15}\text{C} + \text{Pb}$ . Since the  $^{14}\text{C} + n$  c.m. system follows very closely the classical Rutherford trajectory, the impact parameter  $b$  can be related to  $\theta$  by  $b = a \cot(\theta/2) \simeq 2a/\theta$ , where  $a$  is half the distance of the closest approach. Hence, the selection of forward angles, corresponding to large impact parameters can be used to extract the Coulomb breakup component. This method was investigated thoroughly for the case of the  $^{11}\text{Be}$  breakup reaction, where it was successfully used to extract the related  $E1$  component [23].

#### B. Experiment

The experiment was performed at the RIPS facility [28] at RIKEN using the experimental setup shown in Fig. 1 of Ref. [23]. The secondary beam of  $^{15}\text{C}$  was produced by fragmenting  $^{18}\text{O}$  at 100 MeV/nucleon on a 1.1 g/cm<sup>2</sup>-thick Be target. The secondary beam bombarded a 224 mg/cm<sup>2</sup>-thick Pb target. The mean kinetic energy of the incident beam in the Pb target was 68 MeV/nucleon. The momentum width of the secondary beam was  $\pm 0.1\%$ . The energy information of the  $^{15}\text{C}$  ion was obtained event-by-event by time of flight (TOF) measured using two thin plastic scintillators, which were located 4.57 m apart. The trajectory of the  $^{15}\text{C}$  incident ion on the target was determined by four sets of multiwire proportional counters.

The breakup residual particles,  $^{14}\text{C}$  and  $n$ , were emitted in a narrow cone at forward angles with velocities close to that of the  $^{15}\text{C}$  projectile. The neutron was detected by two layers of neutron hodoscope arrays with an effective area of 2.14(W)  $\times$  0.92(H) m<sup>2</sup> placed at 4.60 m and 4.99 m, respectively, downstream of the target. Each array consisted of 15 plastic scintillator rods with 6.1 cm thickness. The angular coverage ranged from  $-7.0^\circ$  to  $19.0^\circ$  in the horizontal direction, and from  $-5.5^\circ$  to  $5.5^\circ$  in the vertical direction. The neutron momentum vector was determined from the TOF and hit position information in the arrays. An intrinsic detection efficiency of 13.4% for the threshold energy of 6.0 MeVee (electron-equivalent energy) was obtained in a separate experiment using the  $^7\text{Li}(p, n)^7\text{Be}$  reaction at 66.7 MeV. The momentum resolutions for the neutron within one  $\sigma$  were 0.99%, 0.36%, and 0.99%, respectively, in  $P_x$ ,  $P_y$ , and  $P_z$  directions in the laboratory frame. Each suffix, here, represents the horizontal, vertical, and parallel(beam) direction, respectively.

The corresponding  $^{14}\text{C}$  particle was analyzed by a magnetic spectrometer equipped with a drift chamber and plastic scintillator hodoscopes. Particle identification was performed by combining  $\Delta E$ , TOF data from the hodoscopes, and magnetic rigidity information from the tracking of the particle. The momentum vector of  $^{14}\text{C}$  was deduced by combining the TOF information with the tracking analysis. The momentum resolutions within one  $\sigma$  were 0.76%, 0.76%, and 2.4%, respectively, in  $P_x$ ,  $P_y$ , and  $P_z$ , in the laboratory frame. The relative energy resolution was estimated by a Monte Carlo simulation incorporating these momentum resolutions, and was found to be well approximated by  $\Delta E_{\text{rel}} = 0.23\sqrt{E_{\text{rel}}}$  MeV( $1\sigma$ ).

### IV. RESULTS AND DISCUSSION

#### A. Energy spectra of breakup cross sections

Figure 1 shows the relative energy spectrum of  $^{14}\text{C} + n$  in the breakup of  $^{15}\text{C}$  on the Pb target. The solid squares show the breakup cross section integrated over the scattering angular range  $0^\circ \leq \theta \leq 6.0^\circ$  which nearly corresponds to the whole acceptance of the present setup. Open circles show the cross section for a selected angular range,  $0^\circ \leq \theta \leq 2.1^\circ$ . The cut at 2.1 degrees is equivalent to an impact parameter of 20 fm. The breakup cross sections, integrated up to  $E_{\text{rel}} = 4$  MeV are  $670 \pm 14(\text{stat.}) \pm 40(\text{syst.})$  mb and  $294 \pm 12(\text{stat.}) \pm 18(\text{syst.})$  mb for  $0^\circ \leq \theta \leq 6.0^\circ$  and  $0^\circ \leq \theta \leq 2.1^\circ$ , respectively. The systematic uncertainties are mainly due to the neutron detection efficiency, which affects the overall normalization of the spectrum. Large breakup cross sections on a heavy target due to Coulomb breakup are typical for loosely bound halo nuclei. However, the  $^{15}\text{C}$  breakup cross section is about  $1/5 \sim 1/3$  of that for conventional halo nuclei such as

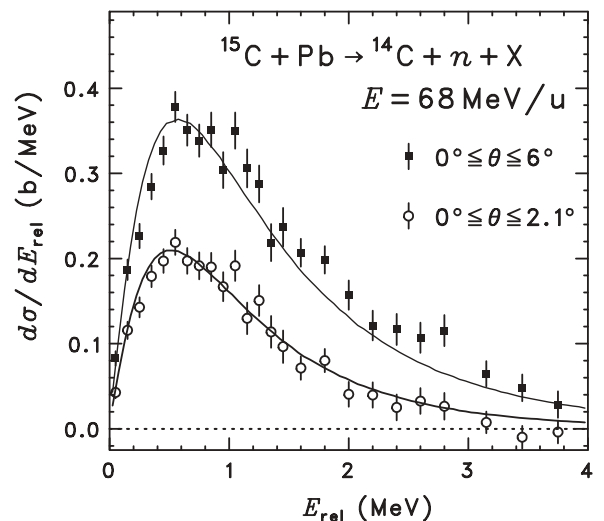


FIG. 1. Breakup cross section as a function of relative energy,  $E_{\text{rel}}$ , of  $^{14}\text{C} + n$  in the reaction  $^{15}\text{C} + \text{Pb}$ . Solid squares represent the data for scattering angles up to 6 degrees, and open circles represent the data for selected scattering angles up to 2.1 degrees. Solid curves are calculations for a direct breakup model with a spectroscopic factor  $\alpha^2 = 0.91$ , for the halo configuration ( $a = 0.5$  fm and  $r_0 = 1.223$  fm). See text for details.

TABLE I. Comparison of spectroscopic factors obtained from different reactions. Two different diffuseness parameters,  $a = 0.5$  fm and  $a = 0.7$  fm, have been used to derive the related spectroscopic factor  $\alpha^2$ . As long as the same  $a$  parameter is used, we find that the result of the current Coulomb breakup experiment is in good agreement with the results of other measurements.

Reaction	$E/A$ (MeV)	References	$a$	$r_0$	$\alpha^2$
Coulomb breakup	68	Present	0.5	1.223	0.91(6)
			0.7	1.25	0.72(5)
Coulomb breakup	605	[11]	0.7	1.25	0.73(5)
			0.5	1.15	0.92(7)
$1n$ removal	103	[16]	0.5	1.223	0.88(4)(5)
$^{14}\text{C}(d, p)^{15}\text{C}$	7	[29,30]			0.88

$^{11}\text{Be}$  [23],  $^{19}\text{C}$  [26], and  $^{11}\text{Li}$  [24], when measured at similar incident energies. This indicates that the size of the halo in  $^{15}\text{C}$  is not as extended as in those known halo nuclei.

The results of the calculations based on first-order perturbation theory (equivalent photon method) combined with the direct breakup mechanism for the two angular ranges are compared with the data in Fig. 1. The matrix element in the direct breakup can be written as

$$\frac{dB(E1)}{dE_{\text{rel}}} = \left| \langle \mathbf{q} | \frac{Ze}{A} r Y_m^1 | \Phi(\mathbf{r}) \rangle \right|^2$$

$$\propto \alpha^2 \left| \langle \mathbf{q} | \frac{Ze}{A} r Y_m^1 | ^{14}\text{C}(0^+) \otimes \nu 2s_{1/2} \rangle \right|^2, \quad (4)$$

where  $\Phi(\mathbf{r})$  stands for the wave function of  $^{15}\text{C}$  and the final state  $\langle \mathbf{q} |$  describes a neutron in the continuum.  $\alpha^2$  represents the spectroscopic factor for the halo configuration  $|^{14}\text{C}(0^+) \otimes \nu 2s_{1/2}\rangle$ , which is the fraction of this configuration in the ground state wave function of  $^{15}\text{C}$ . If the wave function  $\langle \mathbf{q} |$  is assumed to be a plane wave, the first equation represents the Fourier-Bessel transform of the ground state wave function, and the low-energy peak in the  $E1$  spectrum is determined solely by the amplitude of the wave function at large distances. This causes only the  $s$ -wave component, namely the halo configuration, in  $^{15}\text{C}$  to be retained in the second equation.

In the present calculation, the wave function for the halo configuration,  $|^{14}\text{C}(0^+) \otimes \nu 2s_{1/2}\rangle$ , was obtained using a two-body potential model for  $^{14}\text{C}$ -neutron interaction. A Woods-Saxon potential with a radius parameter  $r_0 = 1.223$  fm and a diffuseness parameter  $a = 0.50$  fm was used. The same parameters were used by Terry *et al.* [16] for extracting the spectroscopic factor in the neutron removal reaction of  $^{15}\text{C}$  on a  $^9\text{Be}$  target. They extracted these parameters to adjust the radius obtained in mean field Hartree-Fock (HF) calculation. The potential depth necessary to bind an  $s$ -wave neutron by 1.218 MeV is  $V_0 = 55.4$  MeV. The same potential well is used to calculate the outgoing distorted wave in the continuum and ultimately the matrix element of Eq. (4). A spin-orbit potential  $V_{\text{SO}} = 6.5$  MeV was included in that case.

An excellent agreement between the direct breakup calculation and the spectra, selected for the smaller angular region  $0^\circ \leq \theta \leq 2.1^\circ$ , is obtained using  $\alpha^2 = 0.91(6)$ . This value was deduced by fitting the data to the calculation up to  $E_{\text{rel}} = 1.5$  MeV. The same  $\alpha^2$  can also describe the overall shape and amplitude of the spectra for  $0^\circ \leq \theta \leq 6.0^\circ$ , although some

deviation appears in that case. This could be attributed to higher order effects in the reaction mechanism as well as to some nuclear breakup contribution, as found for the case for  $^{11}\text{Be}$  [23].

We also repeated the calculations using a larger diffuseness parameter  $a = 0.7$  fm and  $r_0 = 1.25$  fm, which were used in the primary analysis for the Coulomb breakup at GSI [11]. In this case, we found about 20% smaller value of  $\alpha^2 = 0.72(5)$ , consistent with the value derived from the GSI experiment. Note that the calculated spectral shapes are found to be almost identical, independent of the choice of potential parameters.

The higher  $\alpha^2$  value ( $\alpha^2 = 0.91(6)$ ), obtained with  $a = 0.50$  fm, is in better agreement with the value of Terry *et al.* [16], as can be seen in Table I. This spectroscopic factor is also consistent with the value obtained from the  $(d, p)$  reaction [29,30]. The Coulomb breakup reaction at GSI also reproduces a larger spectroscopic factor when the analysis is done using similar  $a$  and  $r_0$  parameters. We note that in comparing  $\alpha^2$  values, it is natural to use the same potential parameters. Hereafter, we adopt the higher value of  $\alpha^2 = 0.91$  for consistent discussion with the results of Terry *et al.*, obtained with the same  $a$  and  $r_0$  values.

The quenching of the observed spectroscopic factor with respect to the theoretical values due to short-range correlation effects has been studied by Terry *et al.* [16] and by Gade *et al.* [17]. Their systematic study shows that the quenching factor is close to unity in the case of a loosely bound nucleus such as  $^{15}\text{C}$ . Since the core of  $^{15}\text{C}$  is  $^{14}\text{C}$ , whose structure is dictated by the  $N = 8$  neutron shell closure, the theoretical spectroscopic factor is 0.983. An observed  $\alpha^2$  value close to 0.9 thus implies a reduction factor of about 0.9, as already discussed [16]. From this analysis we can conclude that Coulomb breakup reactions certainly offer a useful tool in understanding spectroscopic factors and their reduction factors, in particular for loosely-bound systems.

## B. $B(E1)$ spectrum

Figure 2 shows the  $B(E1)$  spectrum, which has been extracted from the energy spectrum of the breakup cross section for  $0^\circ \leq \theta \leq 2.1^\circ$  using Eq. (1). The direct breakup model calculation, obtained with  $\alpha^2 = 0.91$  ( $a = 0.5$  fm,  $r_0 = 1.223$  fm), is shown in comparison with the experimental data. Calculations performed with and without incorporating the experimental resolution are shown. The model calculation

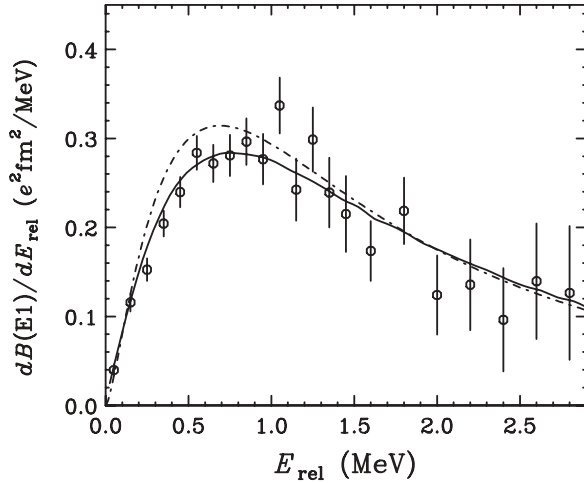


FIG. 2. Extracted  $B(E1)$  spectrum for  $^{15}\text{C}$  excitation. Solid curve corresponds to the direct breakup model calculation. The dot-dashed curve is the same calculation, before folding with the experimental resolution.

is in good agreement with the data, as expected from the agreement of the breakup cross section for  $0^\circ \leq \theta \leq 2.1^\circ$  shown above in Fig. 1.

The  $B(E1)$  value of the current Coulomb breakup spectrum, integrated up to the adiabatic cutoff energy [21]  $E_{\text{rel}}^{\text{max}} = 2.6$  MeV is  $B(E1) = 0.527 \pm 0.045 e^2 \text{ fm}^2$ .  $E_{\text{rel}}^{\text{max}}$  is equal to  $\hbar v \gamma / b$  where  $v$  is the incident velocity of  $^{15}\text{C}$  and  $\gamma$  is the Lorentz  $\gamma$  factor. Note that the  $E1$  virtual photon number for  $E_{\text{rel}} \geq E_{\text{rel}}^{\text{max}}$  decreases drastically, so the extraction of the  $B(E1)$  spectrum above  $E_{\text{rel}}^{\text{max}}$  becomes statistically difficult. We then apply the following non-energy-weighted cluster sum rule to the present case [31]. The sum rule is described as

$$B(E1) = (3/4\pi)(Ze/A)^2 \langle r^2 \rangle, \quad (5)$$

where  $Z$  and  $A$  are the atomic and mass numbers of  $^{15}\text{C}$ , and  $\langle r^2 \rangle$  represents the mean square distance between the valence neutron and the core. Compared to the  $^{11}\text{Be}$  case [23,25], the  $B(E1)$  spectrum of  $^{15}\text{C}$  has a longer tail toward higher excitation energies. Hence, we use the extrapolated values along the solid curve shown in Fig. 2 to extract  $\sqrt{\langle r^2 \rangle} = 4.5(2)$  fm, obtained with a  $B(E1)$  value of  $0.774(67) e^2 \text{ fm}^2$ . This value is large compared to the size of the  $^{14}\text{C}$  core (2.30(7) fm [32]), but significantly smaller than the size extracted for  $^{11}\text{Be}$  (5.77(16) fm [23] and 5.7(4) fm [27]).

### C. Neutron capture cross section

By applying the principle of detailed balance [Eq. (3)] and the relation between  $\sigma_{\gamma n}$  and  $B(E1)$  [Eq. (1)], the neutron capture cross section  $\sigma_{n\gamma}$  can be extracted from the  $B(E1)$  spectrum. The result is shown in Fig. 3. An excellent agreement is obtained with the  $p$ -wave direct radiative capture model calculation [5], up to  $E_{\text{c.m.}} (= E_{\text{rel}}) = 3$  MeV. The  $p$ -wave direct capture corresponds to the direct Coulomb breakup. This result is consistent with the consideration that the final state of the  $^{14}\text{C}$  capture reaction has a halo state with a dominant  $s$ -wave component.

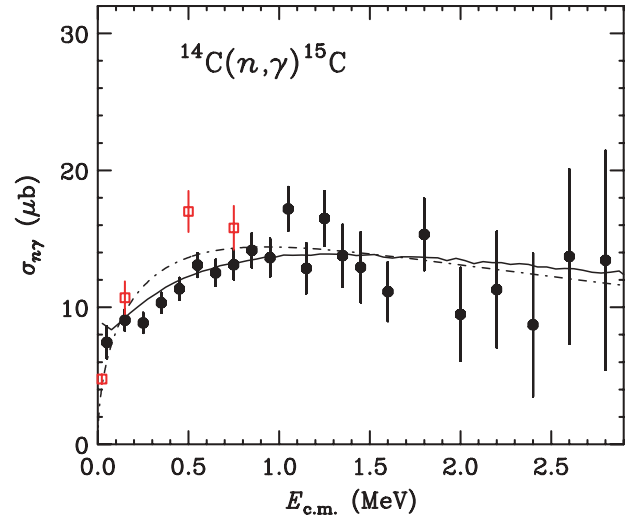


FIG. 3. (Color online) Neutron capture cross section on  $^{14}\text{C}$  leading to the  $^{15}\text{C}$  ground state. Solid black circles are the results of the current experiment, and the red open squares are those from the most recent direct capture measurement [12]. The dot-dashed curve is the calculation based on the direct radiative capture model, while the solid curve is the same one which includes experimental resolution. Both calculations were done using a spectroscopic factor  $\alpha^2 = 0.91$  and with potential parameters  $a = 0.5$  fm and  $r_0 = 1.223$  fm.

In comparison with the most recent direct capture measurement results [12], a good agreement is achieved with only a slight deviation at around  $E_{\text{c.m.}} \sim 0.5$  MeV. The MACS value at  $kT = 23.3$  keV extracted from the current experiment is  $6.1(5) \mu\text{b}$ , compatible with the value of  $7.1(5) \mu\text{b}$ , obtained from the direct measurement [12]. The overall agreement of the Coulomb breakup result with the direct capture measurement suggests that the Coulomb breakup can be a good alternative tool for obtaining the neutron capture cross sections involving radioactive nuclei. Note that in general the Coulomb breakup method can be applied to neutron-rich nuclei where the corresponding direct neutron capture measurement is not feasible.

In comparison with other previous results, we find that only the data obtained from the Coulomb breakup measurement performed at GSI [11] is consistent with the present measurement. The neutron capture cross section derived from the Coulomb breakup experiment performed at MSU [10] is significantly smaller (about  $1 \mu\text{b}$  at  $E_{\text{c.m.}} = 23.3$  keV, and  $4 \mu\text{b}$  around 0.05–0.10 MeV). The result of the first direct measurement [8] was also much smaller (MACS =  $1.72(43) \mu\text{b}$  at  $kT = 23.3$  keV), but some problems related to that very first measurement have been clarified in detail in the most recent direct measurement [12], and the updated values are now in agreement with the present experiment.

As our results are consistent with those of Reifarth *et al.* [12], the argument and implications on the nucleosynthesis scenario follows closely those of Ref. [12], where the role of the  $^{14}\text{C}(n, \gamma)^{15}\text{C}$  in the neutron induced CNO cycles, and the impact of such a cycle on the neutron flux were discussed. By

confirming the direct capture measurement with the present Coulomb breakup result, we expect that a firm discussion on the stellar reactions will make progress.

We add here a short remark on the resonant contribution to the capture rate for the known state at  $E_{c.m.} = 1.885$  MeV with  $J^\pi = 1/2^+$ , discussed by Wiescher *et al.* [4]. The capture rate for this contribution was obtained using a neutron width  $\Gamma_n = 42$  keV and a  $\gamma$  width  $\Gamma_\gamma = 4$  eV, concluding that this resonant contribution is negligibly small compared to the direct capture component. Our estimate, using a fit to the cross section data for  $0^\circ \leq \theta \leq 2.1^\circ$  in Fig. 1, results in an even smaller upper limit of  $\Gamma_\gamma = 1.3$  eV with 95% confidence level, lowering further the influence of this negligible contribution to the capture rate.

## V. CONCLUSION

We have studied the Coulomb breakup of  $^{15}\text{C}$  to extract the  $^{14}\text{C}(n, \gamma)$  cross section and to resolve an otherwise controversial situation. We have found that the  $\sigma_{n\gamma}$  follows the typical  $p$ -wave direct capture behavior, characterized approximately by a  $\sqrt{E_{c.m.}}$  energy dependence of the cross section. Our data shows that the capture cross section is larger by about a factor of four when compared to the value obtained from the early direct neutron capture experiment [8], and

consistent with the most recent measurement [12]. The spectral shape and the amplitude obtained in the present experiment are consistent with a similar measurement performed at GSI, at high incident energies [11]. Meanwhile, the present result shows a disagreement with previous data obtained at MSU [10]. We conclude that this is a typical example of the  $p$ -wave direct capture mechanism, due to loosely-bound halo structure for the final state. This study shows that in the region of neutron-rich nuclei, where important nucleosynthesis paths are located, the  $p$ -wave capture reaction may often dominate over the ordinary  $s$ -wave neutron capture. We also could demonstrate that the Coulomb breakup is a useful tool to extract the corresponding radiative capture cross section, by showing a rare case in which both reactions,  $(n, \gamma)$  and  $(\gamma, n)$ , could be measured.

## ACKNOWLEDGMENTS

Sincere gratitude is extended to the accelerator staff of RIKEN for their excellent operation of the beam delivery. The present work was supported in part by a Grant-in-Aid for Scientific Research (No. 15540257) from the Ministry of Education, Culture, Sports, Science and Technology (MEXT, Japan).

- 
- [1] M. Wiescher, J. Görres, and H. Schatz, *J. Phys. G: Nucl. Part. Phys.* **25**, R133 (1999).
  - [2] M. Terasawa *et al.*, *Astrophys. J.* **562**, 470 (2001).
  - [3] T. Sasaqui *et al.*, *Astrophys. J.* **634**, 1173 (2005).
  - [4] M. Wiescher, J. Görres, and F. K. Thielemann, *Astrophys. J.* **363**, 340 (1990).
  - [5] A. Mengoni, T. Otsuka, and M. Ishihara, *Phys. Rev. C* **52**, R2334 (1995).
  - [6] Y. Nagai *et al.*, *Astrophys. J.* **372**, 683 (1991).
  - [7] T. Ohsaki *et al.*, *Astrophys. J.* **422**, 912 (1994).
  - [8] H. Beer *et al.*, *Astrophys. J.* **387**, 258 (1992).
  - [9] P. Descouvemont, *Nucl. Phys.* **A675**, 559 (2000).
  - [10] Á. Horváth *et al.*, *Astrophys. J.* **570**, 926 (2002).
  - [11] U. Datta Pramanik *et al.*, *Phys. Lett.* **B551**, 63 (2003); U. Datta Pramanik *et al.*, *Prog. Theor. Phys. Suppl.* **146**, 427 (2002).
  - [12] R. Reifarth *et al.*, *Phys. Rev. C* **77**, 015804 (2008).
  - [13] N. K. Timofeyuk, D. Baye, P. Descouvemont, R. Kamouni, and I. J. Thompson, *Phys. Rev. Lett.* **96**, 162501 (2006).
  - [14] N. C. Summers and F. M. Nunes, *Phys. Rev. C* **78**, 011601(R) (2008).
  - [15] T. Nakamura *et al.*, *Nucl. Phys.* **A722**, 301c (2003).
  - [16] J. R. Terry *et al.*, *Phys. Rev. C* **69**, 054306 (2004).
  - [17] A. Gade *et al.*, *Phys. Rev. C* **77**, 044306 (2008).
  - [18] T. Motobayashi *et al.*, *Phys. Rev. Lett.* **73**, 2680 (1994); N. Iwasa *et al.*, *J. Phys. Soc. Jpn.* **65**, 1256 (1996).
  - [19] N. Iwasa *et al.*, *Phys. Rev. Lett.* **83**, 2910 (1999).
  - [20] F. Schümann *et al.*, *Phys. Rev. Lett.* **90**, 232501 (2003).
  - [21] J. D. Jackson, *Classical Electrodynamics*, 2nd ed. (John Wiley & Sons, New York, 1975).
  - [22] C. Bertulani and G. Baur, *Phys. Rep.* **163**, 299 (1988).
  - [23] N. Fukuda *et al.*, *Phys. Rev. C* **70**, 054606 (2004).
  - [24] T. Nakamura *et al.*, *Phys. Rev. Lett.* **96**, 252502 (2006).
  - [25] T. Nakamura *et al.*, *Phys. Lett.* **B331**, 246 (1994).
  - [26] T. Nakamura *et al.*, *Phys. Rev. Lett.* **83**, 1112 (1999).
  - [27] R. Palit *et al.*, *Phys. Rev. C* **68**, 034318 (2003).
  - [28] T. Kubo *et al.*, *Nucl. Instrum. Methods B* **70**, 309 (1992).
  - [29] J. D. Goss *et al.*, *Phys. Rev. C* **12**, 1730 (1975).
  - [30] F. Ajzenberg-Selove, *Nucl. Phys.* **A523**, 1 (1991).
  - [31] H. Esbensen and G. F. Bertsch, *Nucl. Phys.* **A542**, 310 (1992).
  - [32] A. Ozawa, T. Suzuki, and I. Tanihata, *Nucl. Phys.* **A693**, 32 (2001).